

Electronic Supplementary Information

Dynamic Investigation of Interface Atom Migration during Heterostructure Nanojoining

Sen Mei^a, Longbing He^a, Xing Wu^a, Jun Sun^a, Binjie Wang^{a,b}, Xiaochuan Xiong^c and Litao Sun^{*a}

Electron beam irradiation

The electron irradiation might slightly increase the temperature of oxide layer of nanorods. In our experiments, all electrochemically etched metal nanorods were covered with a thin layer of metal oxide. Typically, metal possess excellent thermal conductivity (Al: $238 \text{ Wm}^{-1}\text{K}^{-1}$; Cu: $397 \text{ Wm}^{-1}\text{K}^{-1}$ at room temperature)¹ and the heat generated under electron irradiation can be easily dissipated, so we mainly focused on temperature effect on metal oxide.

According to Fisher's work,^{1,2} the increase of temperature induced by electron irradiation on metal oxide can be estimated as:

$$\Delta T = \frac{I}{4\pi ke} \left(\frac{\Delta E}{d} \right) \left(1 + 2 \ln \frac{b}{r_0} \right) \quad (1)$$

Where I is the beam current, ΔT is the maximum temperature rise caused by an electron beam irradiation, k is the thermal conductivity, ΔE is the total energy loss per electron in a sample of thickness d , b is the radius of the heat sink which is approximately equal to half perimeter of metal nanorod, and r_0 is the radius of area under electron irradiation on nanorod. In our case, for nanorod as cylinder shape b/r_0 is 2, $\Delta E/d$ is considered as a constant of 0.5 eV/nm at 300 keV. Under a magnification of 125kx, I is approximately equal to 10^6 e/nm^2 . The thermal conductivity for Al_2O_3 and CuO are $10 \text{ Wm}^{-1}\text{K}^{-1}$ and $1.6 \text{ Wm}^{-1}\text{K}^{-1}$, respectively.^{3,4} With these parameters, the maximum of temperature rise is about 0.5 K and 3.3 K for Al_2O_3 and CuO, respectively. Therefore, comparing with their melting points (CuO: 1599 K, Al_2O_3 : 2345 K), the electron beam irradiation only induced a slight temperature rise which can be almost neglected.

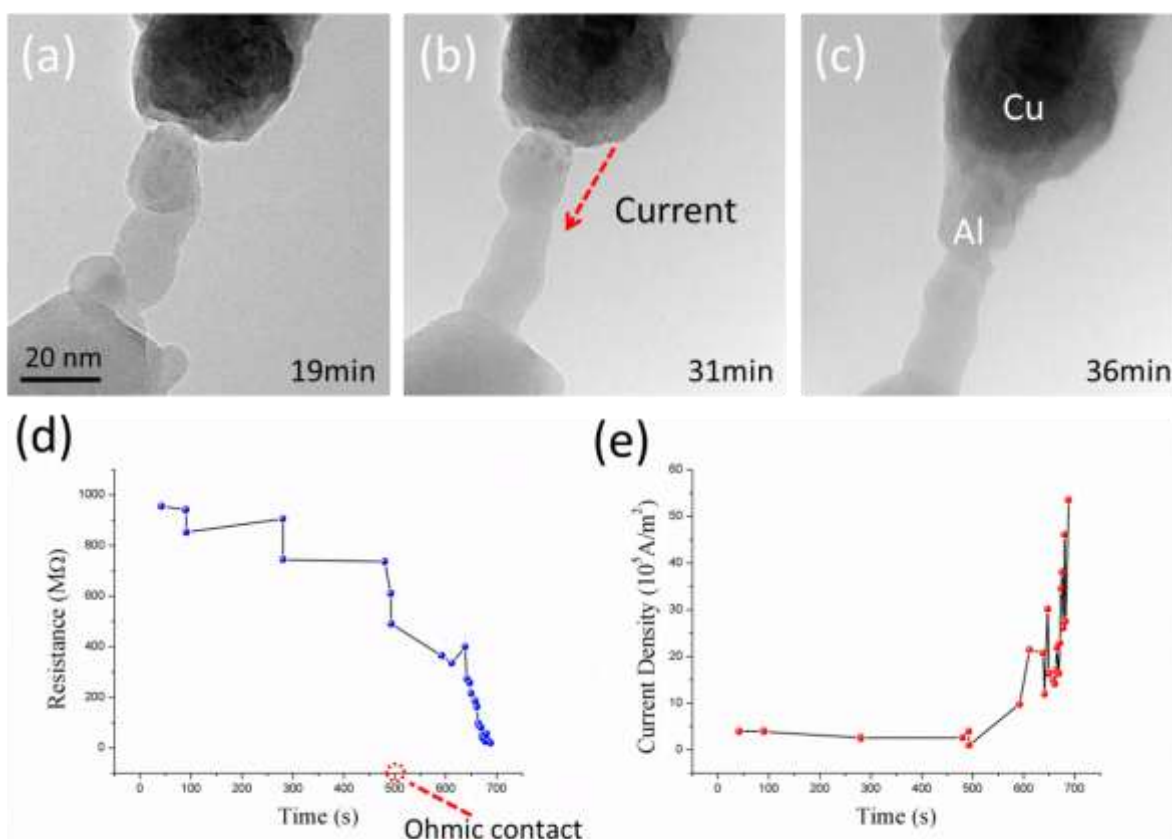


Fig. 1* (a) – (c) Sequence of TEM image of bonding process and the bias was 2 V from Cu to Al. (d) and (e) are the curve of resistance and current density at interface respectively and the 0 sec was set from 23 minutes. As shown in the curves, the ohmic contact was completed on 31 – 32 minutes. After the completion of ohmic contact, the conductivity of the bonding part showed a continuous increase. Please note that, all the data was achieved by discrete electric sweep from +100 mV to -100 mV and the current density was based on +100 mV. The scale bar for (a) – (d) are 20 nm.

As the current density increased, more Joule heat was generated at the interface which naturally facilitated the migration of oxygen atoms. Then the migration of oxygen atoms decreased the resistance and eventually increased current density. As the bias was set to be constant, the increase of current density meant more Joule heat was generated at interface. Therefore, the continuous drop of resistance and increase of current density were caused by this positive feedback process between oxygen atoms' migration and generated Joule heat.

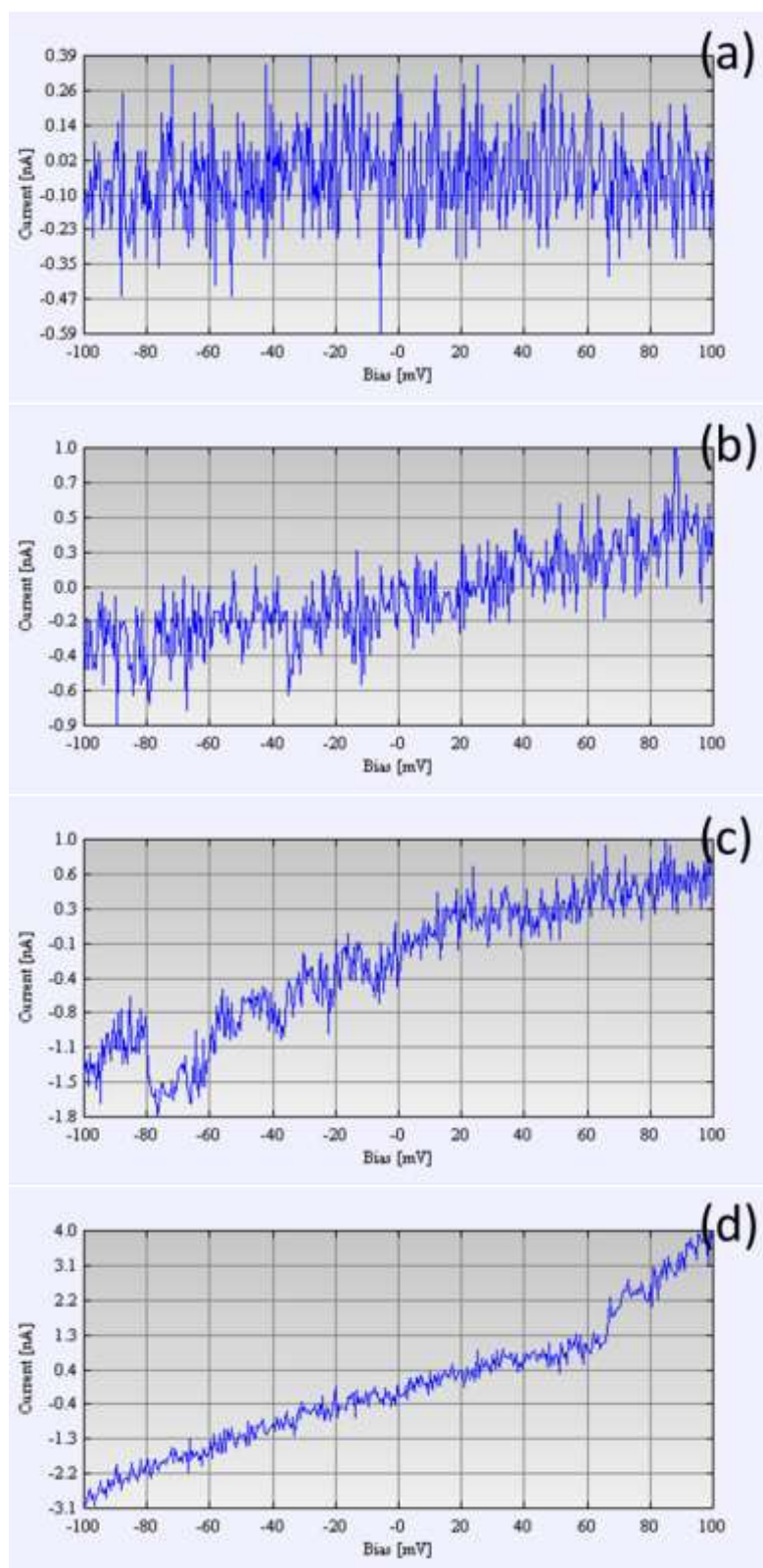


Fig. 2* Electric sweep I-V curves of figure 1* bonding process at different times. (a) 5 min, (b) 19 min, (c) 25 min, (d) 32 min. The positive bias was defined as current flowed from Cu to Al and the electric sweep was set from +100 mV to -100 mV. As the completion of ohmic contact, the I-V curves show more and more smooth profile.

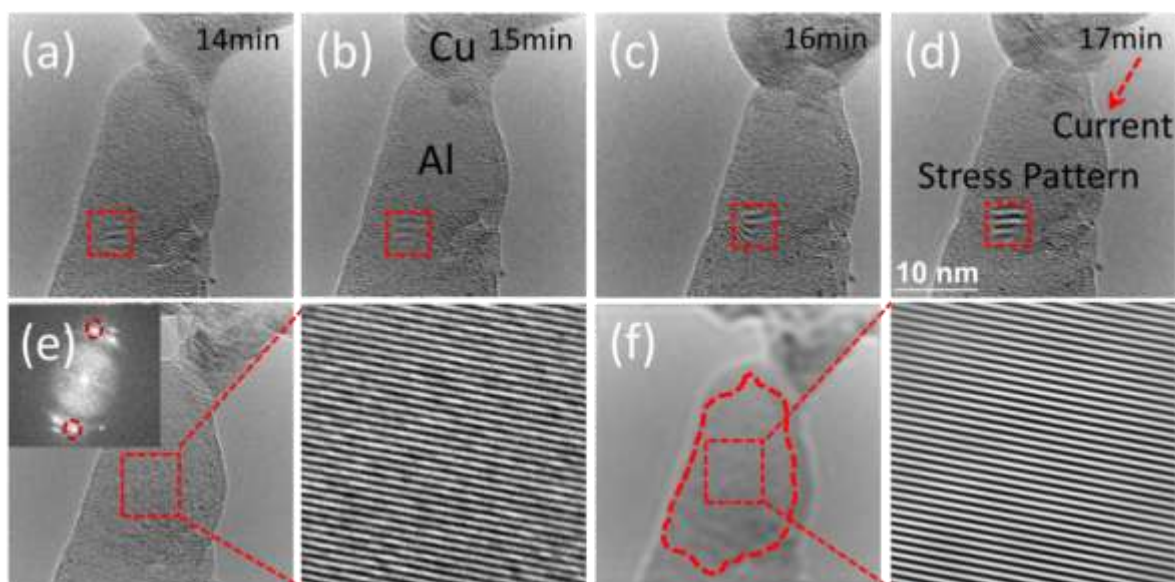


Fig. 3* (a) – (d) Sequence of TEM images show the stress concentration on Al nanorod. The applied bias was 2 V from Cu to Al. (e) The TEM image of contact region before the bias was applied. The inset is FFT (Fast Fourier Transformation) of this image. (f) The filtered image was processed by the selected spots marked in FFT inset indicating the area of single crystal. The lattice spacing is 2.3 Å as (111) crystal plane of Al. The scale bar for (a) – (f) are 10 nm.

The stress pattern could be distinguished from Moiré fringe because high resolution image showed that the concerned region was single crystal, excluding interferences from multiple crystals which might generate Moiré fringes.⁵ It also demonstrates that the stress pattern had become bigger and clearer which indicate a gradually accumulated stress under electrical loadings. Region of stress concentration is near the grain boundary as the stress gradient is always easily generated and accumulated on grain boundaries.

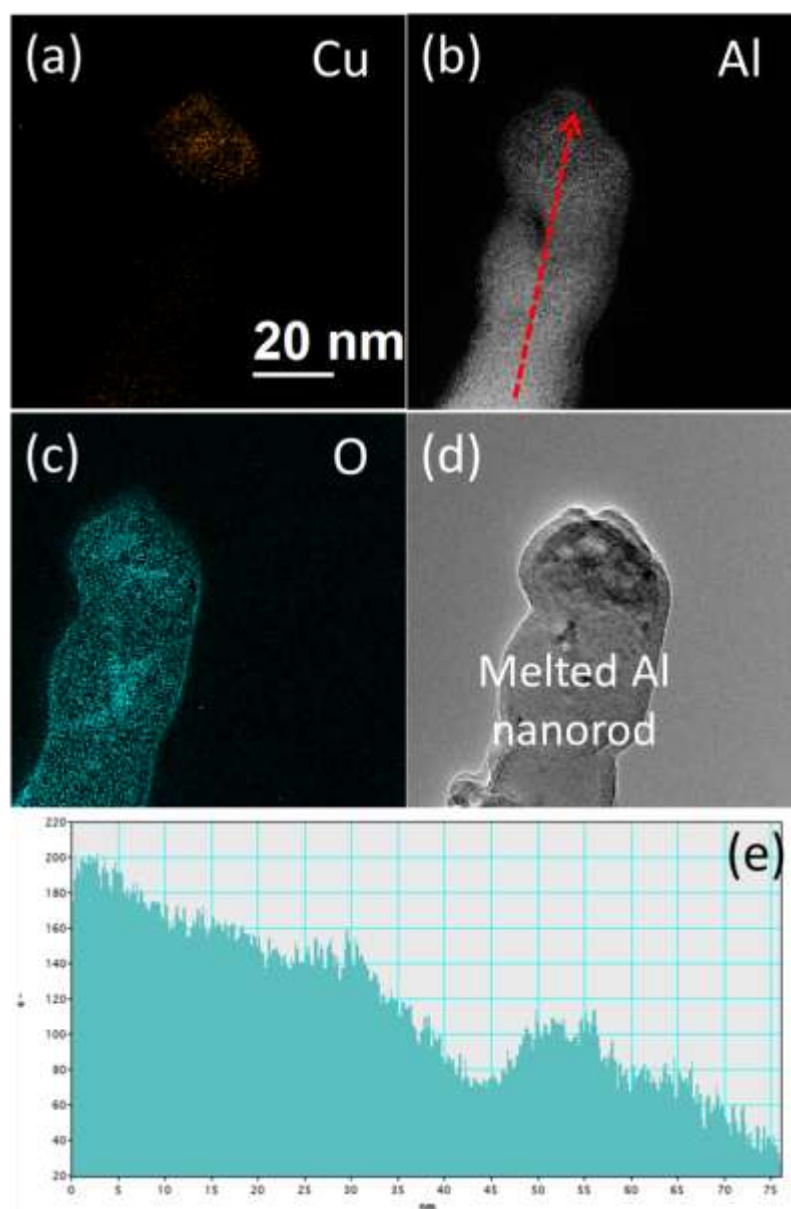


Fig. 4* EFTEM characterization of melted Al nanorod. (a) EFTEM image of Cu for melted Al nanorod. The energy width was set to be 30 eV with a center at 931 eV for Cu. The exposure time range of all the mappings were fixed at 30 seconds. (b) EFTEM image of Al for melted Al nanorod. The energy width was set to be 10 eV with a center at 73 eV for Al. The exposure time range of all the mappings were fixed at 10 seconds. (c) EFTEM image of O for melted Al nanorod. The energy width was set to be 10 eV with a center at 532 eV for oxygen. The exposure time range of all the mappings were fixed at 10 seconds. (d) TEM image of melted Al nanorod. (e) Al signal density along the red arrow in (b). The scale bar for (a) – (d) are 20 nm.

The applied bias was 2 V from Al to Cu and the Al nanorod melted prior to Cu nanorod after 67 minutes' constant bias. As shown in Fig. 4* (a) and (b), the Cu atoms migrated from Cu nanorod were concentrated at the end of Al nanorod which keep in line with the high contrast region in Fig. 4* (d) (the weak noise signal located on bottom in Fig. 4* (a) was caused by multi-scattering).⁵ It also indicated the region where alloy was formed. As shown in Fig. 4* (e), there is an obvious gradient of Al signal density from the end to body region which indicate electromigration process of Al (exclude the influence of thickness as the diameter don't change much along the nanorod in figure's range).

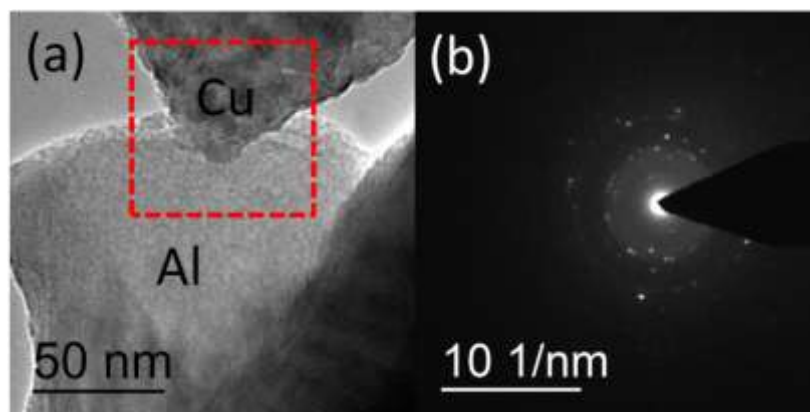


Fig. 5* Selected area electron diffraction (SAED) of contact region. (a) TEM image of contact region. The red rectangle indicates the area of selective diffraction, SAED aperture was set to be 60 nm and spot size was 6. (b) Diffraction image of selected area in (a). Obvious polycrystal ring was observed in diffraction patterns which indicate that contact region was made up of polycrystal.

Notes and references

^a SEU-FEI Nano-Pico Center, Key Lab of MEMS of Ministry of Education, Southeast University, Nanjing, 210096, PR China. Fax: +86-25-83792939; Tel: +86-25-83792632 ext. 8813; E-mail: slr@seu.edu.cn

^b FEI Company, Shanghai Nanoport, No. 690 Bibo Road, Shanghai, 201203, PR China. E-mail: binjie.wang@fei.com

^c General Motors Global Research and Development, China Science Laboratory, 56 Jinwan Road, 201206 Shanghai, China. E-mail: xiaochuan.xiong@gm.com

- 1 S. B. Fisher, *Radiation Effects*, 1970, **5**, 239 – 243.
- 2 I. Jencic, M. W. Bench, I. M. Robertson and M. A. Kirk, *J. Appl. Phys.*, 1995, **78**, 974 – 982.
- 3 A. Kusiak, J. L. Battaglia, S. Gomez, J. P. Manaud and Y. Lepetitcorps, *Eur. Phys. J. Appl. Phys.*, 2006, **35**, 12 – 17.
- 4 B. S. Xu and S. I. Tanaka, *Acta mater.*, 1998, **46**, 5249 – 5257.
- 5 D. B. Williams and C. B. Carter, in *Transmission Electron Microscopy—A Textbook for Materials Science*, Plenum, New York, 1996, vol. 3, pp. 392 – 397.